

Design of a Cherenkov telescope for the measurement of PCR composition above 1 PeV

A S Borisov^{1,a} and V I Galkin^{2,b}

¹*Lebedev Physical Institute of Russian Academy of Sciences,
53 Leninskiy prospekt, Moscow, Russian Federation*

²*Lomonosov Moscow State University Skobeltsyn Institute of Nuclear Physics,
1(2), Leninskie gory, GSP-1, Moscow 119991, Russian Federation*

Abstract. The problem of PCR Composition at super high energies is far from being solved. EAS Cherenkov light spatial-angular distribution (CL SAD) can yield important information on the primary mass. In order to use EAS CL SAD for the study of PCR composition one needs a set of imaging telescopes with the appropriate parameters supported by a dense net of fast optical detectors capable of measuring EAS Cherenkov light pulses. On the basis of full Monte-Carlo simulations the pixel size of imaging telescopes is optimized for a specific observation level ~ 4 km which is typical for the Eastern Pamir mountains.

Another goal to be pursued by the new detector array is the search for ultra high energy gamma ray sources and this is where the imaging technique can help a lot. A simple criterion is introduced to recognize gamma-quanta against the proton background and its performance, once again analyzed using simulated events, sets certain limits to the pixel size.

1 Introduction

Primary cosmic ray composition at super high energies ($E \gtrsim 10^{15}$ eV) is still not studied thoroughly despite many efforts made and resources spent [1]. Probably, the main reason for such a situation is that the sensitivity of the methods used are not adequate to the problem. Thus, we need a method that is really sensitive to the primary mass composition and it looks like we got two of them at hand.

The first method is rather well known one and uses the shape of Cherenkov light lateral distribution (CL LD) at an observation level which strongly correlates with the primary mass for given primary energy and direction. As far as we see, the problem is that in order to get information on the primary mass one should probe CL LDF close to the shower axis (at core distances $R \lesssim 50$ m) which requires a rather dense detector grid which, in turn, limits the detector array area [2]. As long as the main goal of the researcher is to get the largest event statistics possible, irrespective to the quality of the data, this method will never work successfully.

The other method requires even more detailed information on the EAS Cherenkov light as it deals with its spatial-angular distribution and requires very specific optical telescopes to operate. In many aspects

the concept of the method was inherited from the amazing imaging technique of the Cherenkov γ -ray astronomy [3] but CL SAD method has important peculiarities: 1) the background is not so overwhelming and 2) the difference between the events of various origin is smaller. The latter circumstance compels to use a few telescopes observing showers from different core distances to decrease the selection errors [4], which explains the name of the method.

A new "Pamir-XXI" EAS detector array is under development and will be constructed in Eastern Pamir mountains and work under the auspice of the recently established "Pamir-Chacaltaya" international research center. It will study the PCR primary spectrum and composition at $10^{15} - 10^{18}$ eV as well as the nuclear interactions at super high energies. An important part of the array will be a dense grid of fast optical detectors and a few wide-angle telescopes to solve the problem of PCR composition. The rest of the paper describes a calculation made to find out the telescope maximum pixel diameter that makes it possible to distinguish between EAS initiated by protons, nitrogen an iron nuclei. At the same time the idea of probable selection criteria are shown which will be used to process the experimental data.

^ae-mail: asborisov55@mail.ru

^be-mail: v_i_galkin@mail.ru

2 EAS Cherenkov light simulations

Probable observation level of the new array is 4250 m a.s.l. 60 vertical showers for each primary particle (p, N, Fe) of energy 1 PeV were simulated using CORSIKA6.990/QGSJET-I [5]. For each shower the data on CL SAD were stored to 4-dimensional array Q(108,108,250,250) with the first two dimensions forming a square field of view of the telescope ($27^\circ \times 27^\circ$ with $0.25^\circ \times 0.25^\circ$ pixel size, aiming at zenith) and the other two describing the sensitive square at the observation level ($500 \text{ m} \times 500 \text{ m}$ with $2 \text{ m} \times 2 \text{ m}$ square cell). Thus one can use 62500 different positions of a telescope with these data and form grids of pixels of different size.

3 Artificial event processing

In this work four pixel sizes were considered (0.25° , 0.50° , 0.75° , 1.00°) to reveal the dependence of the telescope primary particle selection power on the size. Shower images were chosen at four core distances $R = 50, 100, 150, 200 \text{ m}$. Typical EAS optical image (Fig.1) is a prolate spot with length and width of a few degrees.

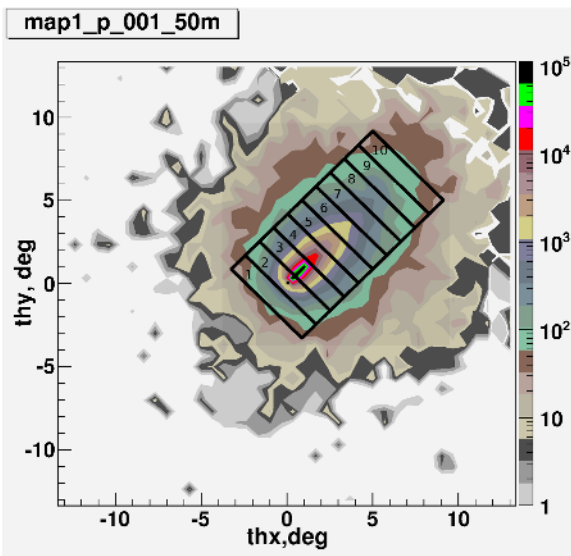


Figure 1. 1 PeV vertical proton shower in the telescope FOV, $R = 50 \text{ m}$. Pixel size: $0.25^\circ \times 0.25^\circ$. Shown in black is the criterion grid which is $5^\circ \times 10^\circ$ rectangle oriented along the long axis of the image. Ten numbered segments of the rectangle are used to form feature vectors for the selection procedure.

To distinguish between different types of primary particles one can use a number of event features including spot length and width widely used in Cherenkov γ -ray astronomy. Here another approach is used based on [4] results: image is integrated over a certain domain (black rectangle in Fig.1) while the integrals over its chips (numbered 1 to 10) present a longitudinal profile of the image. Profiles of EAS from various primary particles differ even though the shower fluctuations some times make them look very

similar. Integration is important for partial suppress of fluctuations but the chips must not be too wide. In this particular case a chip is 5° long ad 1° wide. Image features were formed as partial integral S_i ratios $r_{ij} = S_i/S_j$, $i \neq j$. r_{13} and r_{24} were used in this calculation which does not mean these are the optimum features to be used in the future but still giving about the best separation after a few trials.

These two features form a 2-dimensional feature vector representing every telescope image. 60 feature vectors represent each of the three classes of events (p, N, Fe). Using these three samples a mean feature vector m_i and a covariance matrix Σ_i were calculated for each class $i = p, N, Fe$. For each core distance R and FOV pixel size Bayes normal decision rules minimizing the recognition errors [6] were applied to pairs of classes p-N and N-Fe.

4 Classification results

The results of these classification procedures are shown in Tables 1 and 2 containing the classification errors, i.e. the probabilities to recognize p-event as N-event ($p \rightarrow N$), N-event as p-event ($N \rightarrow p$) and so on. Estimated absolute errors for these data are about 0.02.

We expected that the error would increase with the pixel size substantially because of the digitization errors (when Cherenkov light is distributed over the pixel grid the image is more or less distorted, see Fig.2). The Tables reveal rather weak dependence on pixel size which is presumably due to the better fluctuation suppression in case of large pixels. Still the situation can change with different event features, it should be checked.

The Tables also show a pronounced increase of errors with the core distance. It is due to the steep CL LD at 4250 m observation level for 1 PeV showers but can be partially compensated by a special optimization of event features used for large core distances.

5 Ultra high energy γ -ray event recognition

Optical telescopes under consideration should also enable ultra high energy γ -ray initiated EAS selection against the nuclear EAS background. We analyzed this possibility using two artificial event samples similar to those described above: 80 vertical 50 TeV γ -showers and 80 vertical 100 TeV proton shower observed at 4250 m by the same telescope. The difference in the primary energy is to make up for the different light yield of γ -ray and nuclear showers.

γ -event images deviate substantially from proton event ones, more than the images from different nuclei. Still γ -event selection presents a serious problem because of prevailing (by 3 or 4 orders of magnitude) nuclear event background.

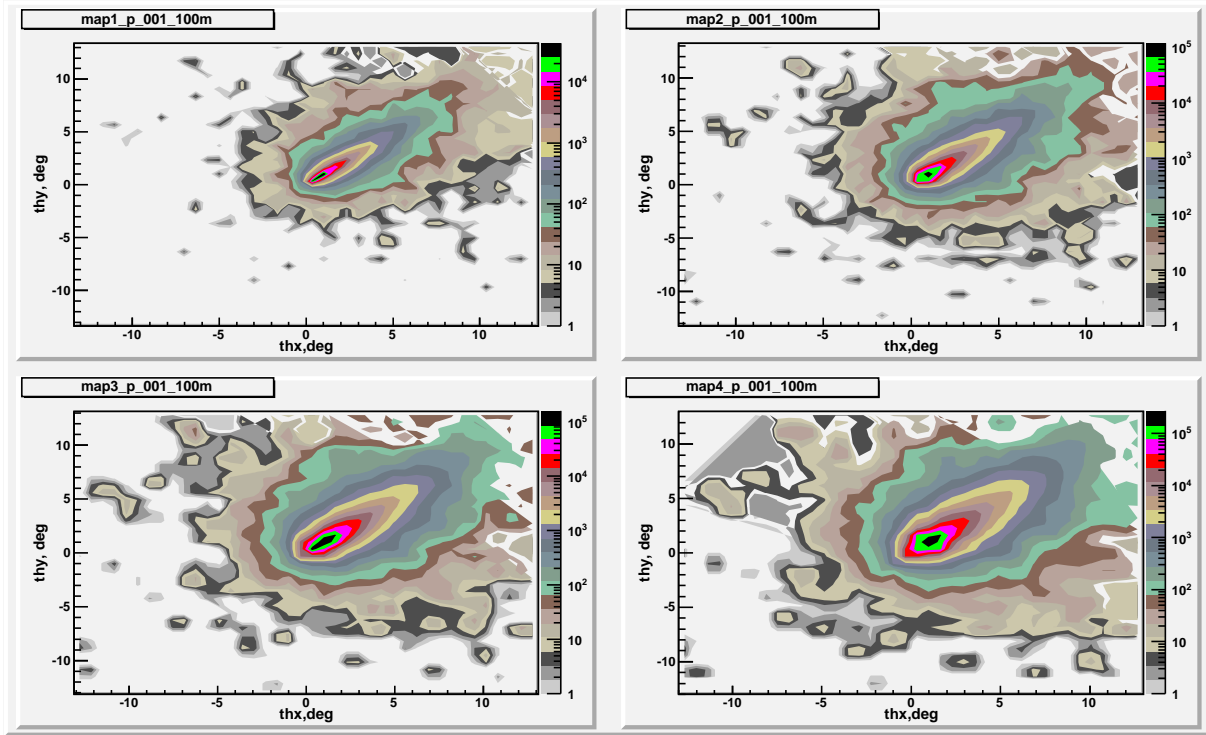


Figure 2. Four image maps for a vertical 1 PeV proton EAS observed from $R = 100$ m at 4250 m a.s.l.; map1 $\leftrightarrow 0.25^\circ \times 0.25^\circ$ pixel size, map2 $\leftrightarrow 0.50^\circ \times 0.50^\circ$ pixel size, map3 $\leftrightarrow 0.75^\circ \times 0.75^\circ$ pixel size, map4 $\leftrightarrow 1.00^\circ \times 1.00^\circ$ pixel size.

Table 1. Recognition errors (misidentification probabilities $P\{p \rightarrow N\}/P\{N \rightarrow p\}$) for different pixel size and core distances.

pixel size	Core distance, m			
	50	100	150	200
$0.25^\circ \times 0.25^\circ$	0.07 / 0.07	0.13 / 0.15	0.20 / 0.20	0.20 / 0.20
$0.50^\circ \times 0.50^\circ$	0.07 / 0.07	0.13 / 0.15	0.20 / 0.20	0.20 / 0.20
$0.75^\circ \times 0.75^\circ$	0.07 / 0.07	0.13 / 0.18	0.20 / 0.22	0.20 / 0.22
$1.00^\circ \times 1.00^\circ$	0.07 / 0.07	0.13 / 0.18	0.20 / 0.22	0.22 / 0.22

Table 2. Recognition errors (misidentification probabilities $P\{N \rightarrow Fe\}/P\{Fe \rightarrow N\}$) for different pixel size and core distances.

pixel size	Core distance, m			
	50	100	150	200
$0.25^\circ \times 0.25^\circ$	0.07 / 0.08	0.13 / 0.18	0.18 / 0.20	0.23 / 0.27
$0.50^\circ \times 0.50^\circ$	0.07 / 0.10	0.13 / 0.20	0.18 / 0.20	0.25 / 0.27
$0.75^\circ \times 0.75^\circ$	0.07 / 0.10	0.15 / 0.20	0.18 / 0.20	0.25 / 0.27
$1.00^\circ \times 1.00^\circ$	0.07 / 0.10	0.15 / 0.20	0.18 / 0.20	0.25 / 0.28

Table 3. Recognition errors (misidentification probabilities $P\{\gamma \rightarrow p\}/P\{p \rightarrow \gamma\}$) for different pixel size and core distances.

pixel size	Core distance, m			
	50	100	150	200
$0.25^\circ \times 0.25^\circ$	0.2875 / 0.0125	0.8000 / 0.0125	0.1750 / 0.0125	0.2250 / 0.0125
$0.50^\circ \times 0.50^\circ$	0.2250 / 0.0125	0.8000 / 0.0125	0.3250 / 0.0125	0.2000 / 0.0125
$0.75^\circ \times 0.75^\circ$	0.2250 / 0.0125	0.7125 / 0.0125	0.6500 / 0.0125	0.5000 / 0.0125
$1.00^\circ \times 1.00^\circ$	0.2750 / 0.0125	0.8875 / 0.0125	0.2075 / 0.0125	0.2000 / 0.0125

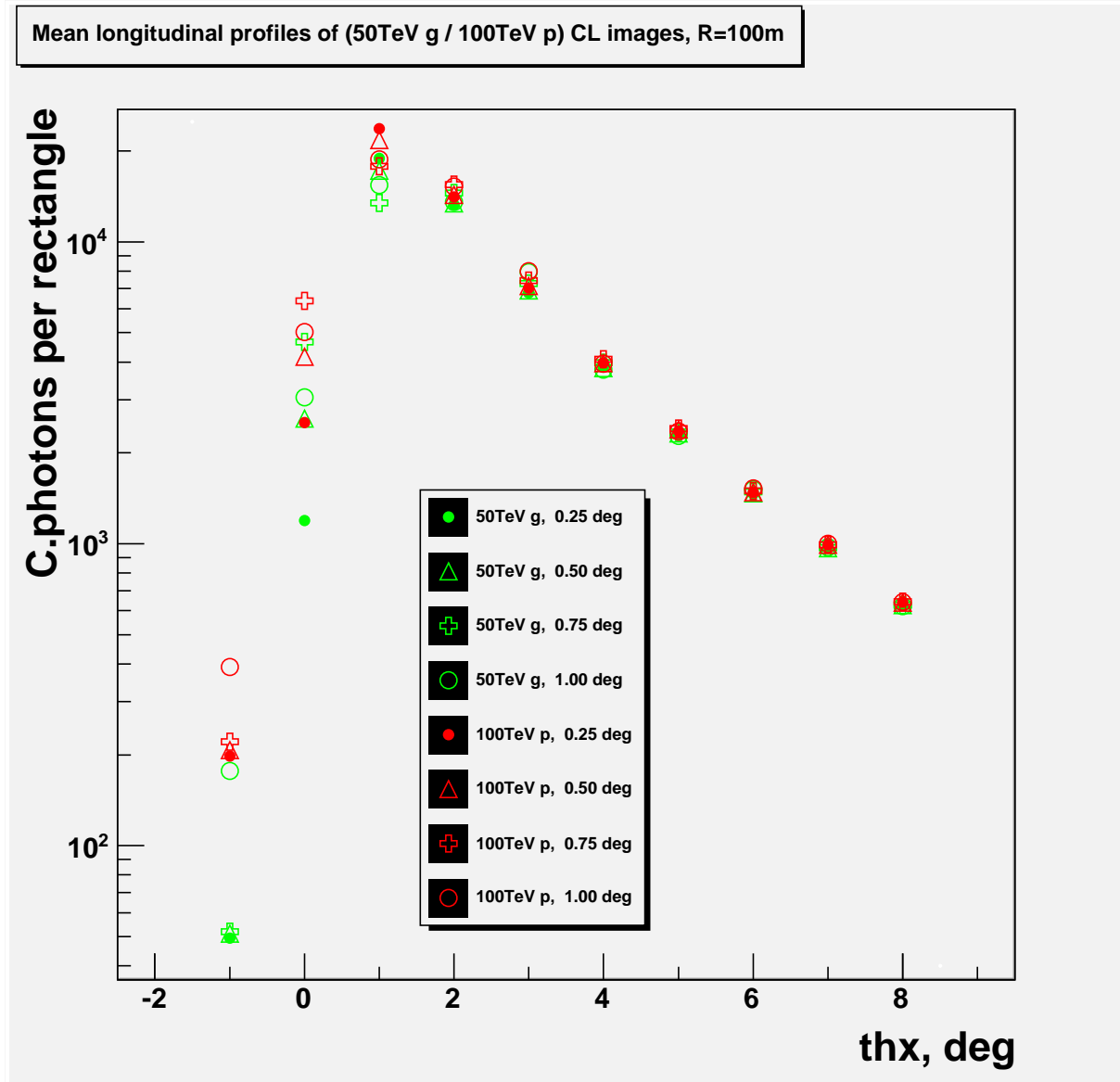
**Figure 3.** Mean longitudinal image profiles for γ -ray and p EAS observed from $R = 100$ m for different pixel size.

Fig.3 presents mean longitudinal image profiles which give us a clue on what ratios should be used in a feature vector to make the selection effective.

The same 2-dimensional feature vector (r_{13}, r_{24}) is used in Bayes normal decision rules, separately for each of 16 combinations of pixel size and core distance. As the main goal of a decision rule is to suppress as many proton events as possible, the rule critical values are tuned in such a way that misidentification probability $P\{p \rightarrow \gamma\}$ becomes 1/80, i.e. only one proton event is recognized as γ -event (Table 3). $P\{\gamma \rightarrow p\}$ probability defines the fraction of signal passing through the filter: $P\{\gamma \rightarrow \gamma\} = 1 - P\{\gamma \rightarrow p\}$.

One can see a pronounced decrease of $P\{\gamma \rightarrow \gamma\}$ at 100 m from the shower core which means that γ -ray and p EAS look rather similar at that core distance. One can also admit that there is no substantial difference between the telescopes with pixel size $0.75^\circ \times 0.75^\circ$ and $1.00^\circ \times 1.00^\circ$ from the point of view of γ -ray event selection either. We should consider some other selection criteria to choose the pixel size but it looks like it may be set to something like $1.00^\circ \times 1.00^\circ$ so that 30° FOV would be covered by about 1000 pixels.

6 Conclusions

Some of the features of the Cherenkov telescopes of "Pamir-XXI" detector array were more or less established by this CL SAD simulation. Their field of view should be about 30° in diameter with effective mirror area 3-4 m² and pixel size $0.75^\circ \times 0.75^\circ$ to $1.00^\circ \times 1.00^\circ$. Using a set of a few such instruments, supported by a dense (with ~ 30 m step) net of fast optical detectors, the detector array will be able to tell different groups of primary nuclei from one another at energies above 100 TeV and, very probably, to select UHE γ -quanta against the nuclear background.

7 Acknowledgement

This work is supported by the Ministry of Education and Science of the Russian Federation (state contracts No. 11.519.11.5022 and No. 16.518.11.7063).

References

- [1] Antoni T, Apel W D, Badea A F, et al. 2005 *Astropart. Phys.* **24** 1-25
 Aglietta M, Alessandro B, Antonioli P, et al. 2004 *Astropart. Phys.* **21** 583-596
 Fowler J W, Fortson L F, Jui C C H, et al. 2001 *Astropart. Phys.* **15** 49-64
 Arqueros F, Barrio J A, Bernlohr K, et al. 2000 *Astron. Astrophys.* **359** 682-694
 Tsunesada Y, Kakimoto F, Furuhashi F, et al. 2008 *Proc. 30th ICRC (Merida)* **4** 127-130
 Chernov D V, Korosteleva E E, Kuzmichev L A, et al. 2005 *Int. J. Mod. Phys. A* **20** 6799-6801
- [2] Anokhina A M, Antonov R A, Bonvech E A, et al. 2009 *Bull. Lebedev Phys. Inst.* **36** 146
- [3] Weekes T C 1989 *ApJ* **342** 379
- [4] Galkin V I and Dzhatdov T A 2010 *Moscow Univ. Bull.* **65** No3 195-202
 Galkin V I and Dzhatdov T A 2011 *Bull. Rus.Ac.Sci.Phys.* **75** No.3 309-312
- [5] Heck D and Pierog T 2011 *Extensive Air Shower Simulation with CORSIKA: A User's Guide* KARLSRUHER INSTITUT FUR TECHNOLOGIE
- [6] Fukunaga K 1972 *Introduction to statistical pattern recognition* (New York and London: Academic press) p 98